

# Radical tropolone biosynthesis

Tyler J. Doyon,<sup>1,2</sup> Kevin C. Skinner,<sup>1,3</sup> Di Yang,<sup>1,3</sup> Leena Mallik,<sup>2,3</sup> Troy Wymore,<sup>3</sup> Markos Koutmos,<sup>2,3</sup> Paul M. Zimmerman,<sup>3</sup> Alison R. H. Narayan<sup>1,2,3\*</sup>

<sup>1</sup>Life Sciences Institute, University of Michigan, Ann Arbor, Michigan 48109, USA. <sup>2</sup>Program in Chemical Biology, University of Michigan, Ann Arbor, Michigan 48109, USA. <sup>3</sup>Department of Chemistry, University of Michigan, Ann Arbor, Michigan 48109, USA.

\*Corresponding author, email: arhardin@umich.edu

## Abstract

Non-heme iron (NHI) enzymes perform a variety of oxidative rearrangements to advance simple building blocks toward complex molecular scaffolds within secondary metabolite pathways. Many of these transformations occur with selectivity that is unprecedented in small molecule catalysis, spurring an interest in the enzymatic processes which lead to a particular rearrangement. In-depth investigations of NHI mechanisms examine the source of this selectivity and can offer inspiration for the development of novel synthetic transformations. However, the mechanistic details of many NHI-catalyzed rearrangements remain underexplored, hindering full characterization of the chemistry accessible to this functionally diverse class of enzymes. For NHI-catalyzed rearrangements which have been investigated, mechanistic proposals often describe one-electron processes, followed by single electron oxidation from the substrate to the iron(III)-hydroxyl active site species. Here, we examine the ring expansion mechanism employed in fungal tropolone biosynthesis. TropC, an  $\alpha$ -ketoglutarate-dependent NHI dioxygenase, catalyzes a ring expansion in the biosynthesis of tropolone natural product stipitatic acid through an under-studied mechanism. Investigation of both polar and radical mechanistic proposals suggests tropolones are constructed through a radical ring expansion. This biosynthetic route to tropolones is supported by X-ray crystal structure data combined with molecular dynamics simulations, alanine-scanning of active site residues, assessed reactivity of putative biosynthetic intermediates, and quantum mechanical (QM) calculations. These studies support a radical ring expansion in fungal tropolone biosynthesis.

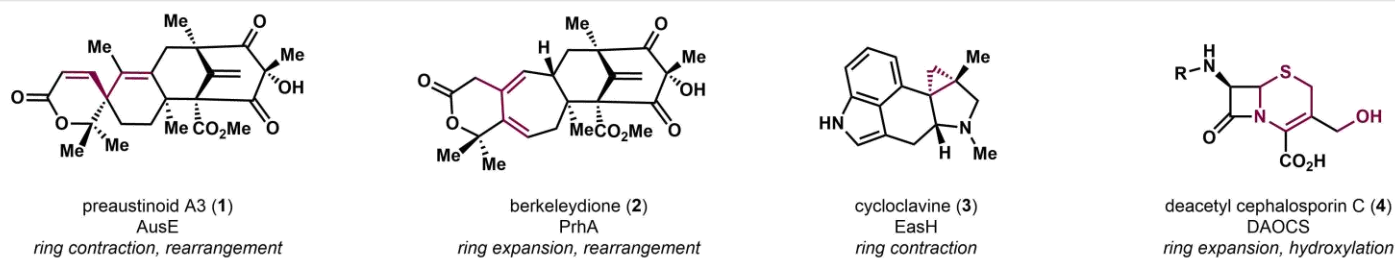
## Introduction

Enzymes catalyze challenging transformations with exquisite control over chemo-, site- and stereoselectivity, directing the synthesis of structurally-complex products from bioavailable starting materials. These transformations often take advantage of the three-dimensional architecture of the enzyme active site to guide reactive intermediates toward formation of the desired product.<sup>1</sup> Biocatalytic control over the fate of reactive intermediates is a common mechanistic archetype in a variety of enzymes such as cyclases, which leverage active site geometries to induce selective cyclization reactions, polyketide synthases that deliver specific products from large, structurally-complex intermediates, Diels-Alderases, which choreograph the relative position of two reactive components to form a stereo-enriched product, and non-heme iron (NHI) dioxygenases, an enzyme class known to catalyze numerous skeletal rearrangements through radical or polar mechanisms.<sup>1-4</sup> In many cases, reactions of identical intermediates generated outside of the enzyme active site proceed in an uncontrolled fashion, leading to racemic products or fundamentally divergent reactivity.<sup>1-2</sup>

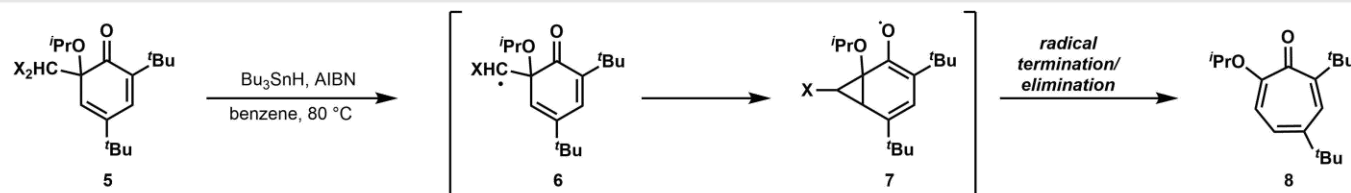
In contrast to the selectivity demonstrated by enzyme-mediated transformations, small molecule-enabled transformations often require careful substrate design to achieve a desired rearrangement, adding synthetic steps and reducing the efficiency and sustainability of the resulting synthesis.<sup>5-6</sup> Radical-based rearrangements are particularly impacted by selectivity challenges, as competing radical pathways often complicate anticipated reaction outcomes.<sup>5-6</sup> As a result, selectivity can be achieved only through optimization of substrate design and reaction conditions to favor the desired reaction pathway.<sup>5-6</sup> In comparison, biocatalysts operate with precise control over the reaction outcome, enabling highly selective and direct synthesis of natural product scaffolds.<sup>7-9</sup> Therefore, thorough examination of the mechanistic details of enzyme-catalyzed rearrangements is critically important to the development of novel, selective approaches to complex molecule synthesis.

Non-heme iron (NHI) enzymes perform an array of oxidative transformations and rearrangements in secondary metabolism.<sup>4, 10-11</sup> Members of the  $\alpha$ -ketoglutarate-dependent family of NHI dioxygenases couple the oxidative decarboxylation of  $\alpha$ -ketoglutarate ( $\alpha$ -KG) to the activation of molecular oxygen, generating an iron(IV)-oxo species (**17**, Fig. 1D).<sup>12-13</sup> Through this common mechanism of oxygen activation, NHI enzymes catalyze a variety of selective transformations that are often initiated by hydrogen atom abstraction, followed by a variety of processes including hydroxylation, desaturation, halogenation, endoperoxidation, epimerization, ring expansion and ring contraction, among others.<sup>4, 11-13</sup> Understanding how the fate of a radical intermediate is controlled by each catalyst has motivated structural, spectroscopic and computational studies of NHI enzymes. In-depth interrogation of NHI-catalyzed reaction mechanisms has revealed critical enzyme-substrate interactions that dictate the reaction outcome in several cases.<sup>7-9</sup> These studies provide mechanistic detail for several NHI-catalyzed rearrangements, including ring contractions and ring expansions.<sup>14-17</sup>

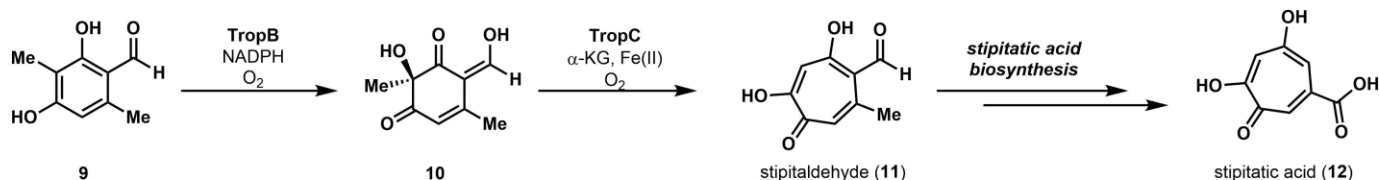
### A. NHI enzyme-catalyzed ring modification



### B. Radical synthesis of tropolones from dearomatized catechols<sup>25-26</sup>



### C. Biosynthesis of tropolone natural product stipitatic acid (12)



### D. This work: Mechanism of fungal tropolone biosynthesis

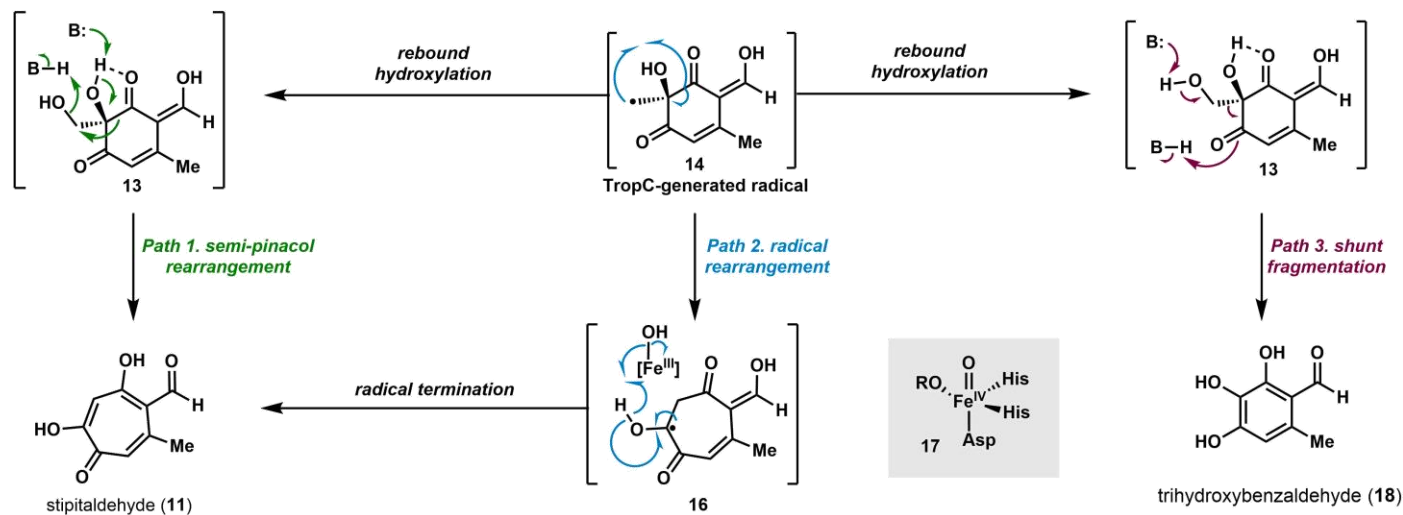


**Figure 1.** A. Ring rearrangement reactions catalyzed by NHI enzymes. B. Radical tropolone synthesis from dearomatized *ortho*-phenols. C. Biosynthesis of stipitaldehyde (11) on path to fungal tropolone natural products. D. This work: Mechanistic studies of ring expansion in NHI enzyme TropC.

Ring-modifying transformations often proceed through an initial C–H atom abstraction, followed by radical rearrangement and termination by single electron oxidation or hydroxylation to yield product.<sup>7-9, 14-17</sup> The NHI active site architecture dictates the reaction outcome by exerting fine control over events downstream from hydrogen atom abstraction, enabling highly selective transformations.<sup>7-9, 14-17</sup> For example, AusE and PrhA are highly related NHI enzymes (78% sequence ID) that catalyze divergent transformations on a common substrate to generate preaustinoide A3 (1) and berkeleydione (2), respectively.<sup>7-9</sup> Structural and computational studies have shown that minor differences in their active site architecture play a critical role in determining the outcome of the initial enzyme-catalyzed desaturation, ultimately leading to the formation of two distinct natural products through a divergent radical rearrangement process.<sup>7, 9</sup> Similar mechanistic studies found that the NHI-catalyzed biosynthesis of cycloclavine (3) and deacetoxy-cephalosporin C (4) proceed through a one-electron reaction pathway, suggesting a common mechanistic archetype for ring rearrangements catalyzed by NHI enzymes.<sup>14-16, 18</sup>

Natural products often possess medium-sized rings (7-11 atoms) which can be difficult to access using small molecule techniques. One such class of synthetically-challenging targets are tropolones, a structurally-diverse group of bioactive metabolites with an aromatic cycloheptatriene core structure containing an  $\alpha$ -hydroxyketone moiety (see Figure 1C, **11**).<sup>19-21</sup> Tropolones have been synthesized through a variety of approaches, typically involving ring expansion.<sup>22</sup> These transformations include classic two-electron rearrangements such as the Büchner reaction,<sup>23</sup> the de Mayo fragmentation<sup>24</sup> and [5+2] cycloadditions.<sup>22</sup> In addition, radical-based approaches have been successful in synthesizing tropolones from *ortho*-dearomatized catechols (**5**) through a selective radical ring expansion mechanism (Figure 1B).<sup>25-26</sup> This approach required pre-functionalization of the arene to ensure that radical initiation occurred at the methyl halide *ipso* to the site of dearomatization, leading to the desired rearrangement (Figure 1B).<sup>25-26</sup> While these methods have been successful in enabling ring expansion, they require arduous synthetic efforts to achieve the desired substitution pattern of the tropolone natural product, preventing facile access to the target compound.<sup>22</sup> In contrast, Nature efficiently assembles complex tropolones using available biosynthetic machinery. In fungi, the identification of the stipitatic acid (**12**) biosynthetic gene cluster in *T. stipitatus* provided a blueprint for the assembly of these aromatic seven-membered rings in Nature (Figure 1C).<sup>21</sup> Fungal tropolone biosynthesis, in the case of stipitatic acid, commences with polyketide synthase production of 3-methylorcinolaldehyde (**9**) and subsequent flavin-dependent monooxygenase-mediated oxidative dearomatization.<sup>21, 27</sup> It has been established that the resulting dienone (**10**) undergoes an oxidative ring expansion catalyzed by an  $\alpha$ -KG-dependent NHI enzyme, TropC, to afford stipitaldehyde (**11**). Downstream enzymatic modifications of stipitaldehyde (**11**) generate stipitatic acid (**12**).<sup>21</sup> Since the identification and characterization of enzymes involved in stipitatic acid biosynthesis, several other tropolone natural products have been shown to proceed through the same oxidative dearomatization/ring expansion cascade to generate the tropolone core.<sup>28-29</sup> Motivated to understand the chemical steps of this powerful transformation, we initiated our studies on the chemistry and mechanism of the TropC-catalyzed ring expansion. In particular, we sought to investigate two transformations which TropC has been shown to catalyze (1) ring expansion to generate stipitaldehyde (**11**) and (2) a fragmentation reaction which produces trihydroxybenzaldehyde (**18**), a known shunt product in fungal tropolone biosynthesis (Figure 1D).

As the fate of a radical intermediate in NHI dioxygenase-catalyzed transformations is critical to the observed reactivity of the enzyme, we envisioned that TropC-catalyzed ring expansion could occur through several possible mechanistic pathways. Cox and coworkers initially proposed that TropC performs a polar ring expansion to produce stipitaldehyde (**11**, Figure 1D, Path 1).<sup>19-21</sup> Their proposal commences with TropC-mediated C–H atom abstraction on dienone **10** to generate radical species **14**.<sup>19-21</sup> Subsequent rebound hydroxylation would afford diol **13**, which is proposed to undergo a semi-pinacol rearrangement to form stipitaldehyde (**11**). We anticipated that this rearrangement could be assisted by residues in the TropC active site through activation of the alcohol leaving group in diol intermediate **13**.<sup>19-21</sup> The proposed ring expansion mechanism is also consistent with the observed formation of a shunt product in this biosynthetic pathway, **18**, which is anticipated to arise through loss of formaldehyde and concomitant rearomatization to produce trihydroxybenzaldehyde **18** (Figure 1D, Path 3).<sup>21</sup> Based on the radical reaction pathways that have been proposed for other ring modifying enzymes, we envisioned an alternative mechanism to arrive at stipitaldehyde in which radical **14** directly undergoes ring expansion, followed by radical termination via a single electron oxidation involving the iron(III)-hydroxyl species (Figure 1D, Path 2). Under this model, the product generated by the enzyme is determined by the radical termination process which occurs in the active site. If rebound hydroxylation predominates, then trihydroxybenzaldehyde (**18**) will be the major product formed. If radical rearrangement is preferred under the reaction conditions, then stipitaldehyde (**11**) formation will dominate. To decipher the ring expansion mechanism used by TropC, we aimed to investigate the active site architecture of the enzyme, as well as the reactivity of proposed ring expansion intermediate **13**.

## Results and discussion

To determine the nature of the TropC-catalyzed ring expansion, we began by performing a computational analysis of the proposed pathways (Figure 1D, Path 1-3). Through these calculations, we aimed to compare the relative barriers of proposed ring expansion pathways to assess the feasibility of a one- or two-electron ring expansion mechanism. Each mechanistic pathway was evaluated using a small molecule NHI mimetic complex (see Supplementary Figure S32). We manually performed tautomerization of reaction pathway products to model stipitaldehyde (**11**) and the trihydroxybenzaldehyde shunt product **18** as protonated, neutral structures, reflecting the enzymatic reaction conditions for TropC-catalyzed ring expansion (pH 7.0). Water molecules were used as proton shuttles to mimic the protonation and deprotonation events that would be facilitated by residues in the enzyme active site.

We began our computational investigations using the radical intermediate **14** (Figure 2), which is the divergence point for each of the pathways along the potential energy surface (PES). We first explored the radical rearrangement (Path 2), which occurs with a barrier of 12.7 kcal/mol (**16**). A subsequent H-atom abstraction by an iron(III)-hydroxyl species to produce the tautomer of stipitaldehyde (**11**) was calculated to be barrierless. This calculation was supported by literature precedent which demonstrated that tropolones could be synthesized from *ortho*-dearomatized radicals (Figure 1B).<sup>22, 26</sup> We then explored the rebound hydroxylation and semi-pinacol rearrangement (Path 1). As expected, rebound hydroxylation to produce diol **13** was found to be a barrierless process in our active site model.<sup>12, 30-31</sup> In an enzyme active site, we anticipate

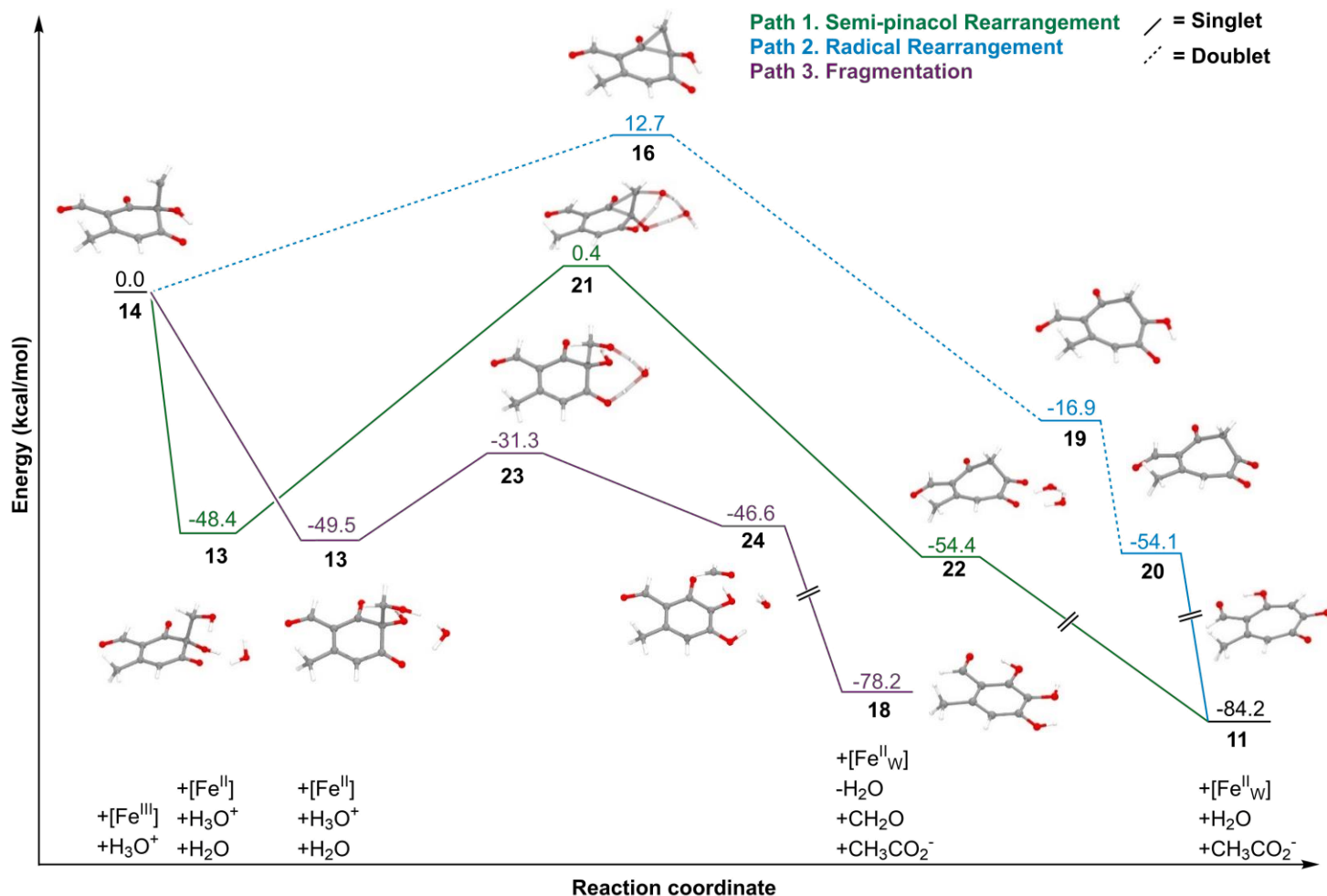


**Figure 2.** QM calculations for TropC-catalyzed reaction pathways to generate stipitaldehyde (**11**) and trihydroxybenzaldehyde **18**.

that substrate movement and alignment would be restricted by local residues, resulting in thermodynamic barriers to this process.<sup>12, 30-31</sup> The barrier for the proposed semi-pinacol rearrangement was observed to be excessively high at 48.8 kcal/mol (**21**), indicating that this transformation is not likely to occur. These barriers are in agreement with computational analysis by Siegbahn and coworkers examining ring expansion mechanisms of *ortho*-dearomatized phenols, indicating that a semi-pinacol type ring expansion is unlikely to occur in these systems.<sup>32</sup> In comparison, fragmentation to afford an aromatic product from diol **13** (Path 3) to produce formaldehyde and trihydroxybenzaldehyde **18** was found to be a low barrier process at 18.2 kcal/mol (**23**). These calculations suggest that diol **13** favorably undergoes fragmentation and rearomatization (Path 3), rather than the proposed semi-pinacol ring expansion (Path 1). The calculated low barrier for Path 3 is supported by experimental observation of trihydroxybenzaldehyde formation during the TropC-catalyzed reaction. Taken together, the QM simulations support our alternative mechanistic proposal in which the radical rearrangement is a kinetically and thermodynamically accessible route towards tropolone formation (Path 2).

Next, we sought experimental evidence to discriminate between the two reaction pathways under consideration for TropC-catalyzed ring expansion. We aimed to further interrogate the proposed ring expansion mechanisms by performing a detailed mutational analysis of TropC in order to determine if specific active site residues are responsible for catalyzing the ring expansion. To gain structural information to guide this work, we obtained TropC crystals using the sitting drop vapor diffusion method (see supplemental information for details). Following data collection, we found that TropC crystallized in the P3<sub>1</sub>21 space group with two molecules of TropC in the asymmetric unit (PDB ID: 6XJJ). The crystal structure of unliganded TropC was solved at a resolution of 2.7 Å with the molecular replacement method using the structure of thymine-7-hydroxylase (T7H) of *Neurospora crassa* as a search model (Figure 3).<sup>33</sup> Our analysis of the structural data indicated that TropC adopts a similar architecture as other  $\alpha$ -KG-dependent NHI dioxygenases<sup>34</sup>. The three-dimensional structure of TropC consists of double-stranded  $\beta$ -helix (DSBH or jelly-roll) fold at the core of the protein<sup>34</sup>. The DSBH core of TropC is comprised of ten anti-parallel  $\beta$ -strands, which form two  $\beta$ -sheets, called major and minor  $\beta$ -sheets. Major  $\beta$ -sheets of TropC include  $\beta$ 1-5,  $\beta$ 8 and  $\beta$ 10, and the minor  $\beta$ -sheet consists of  $\beta$ 6,  $\beta$ 7 and  $\beta$ 9 (Supplementary Figure S29). The exterior of the major  $\beta$ -sheets of the DSBH fold is surrounded by  $\alpha$ -helices ( $\alpha$ 1-3,  $\alpha$ 5 and  $\alpha$ 7) to form a compact globular structure.

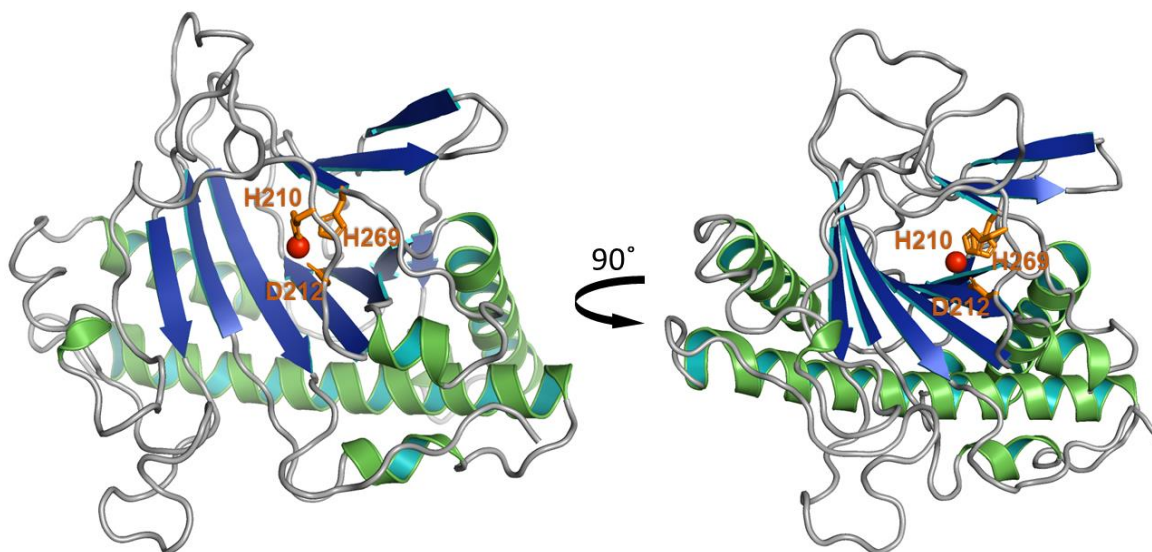


**Figure 3.** Overall architecture of TropC determined using X-ray crystallography (PDB ID: 6XJJ). (Left) Structure of TropC from *T. stipitatus* in ribbon representation. At the core of TropC, the Fe (III) shown with red sphere and side chain of residues, H210, D212 and H269, are shown in stick representation. (Right) Rotated view of crystal structure of TropC and active site located at the center of the protein.

Structures similar to TropC in the Protein Data Bank (PDB) were explored by using the DALI server (Supplementary Table S2),<sup>35</sup> revealing the highly similar structures of isopenicillin N synthase from *Pseudomonas aeruginosa* PAO1 (*Pa/PNS*, PDB ID: 6JYV, Z-score: 32.2)<sup>36</sup> and thymine-7-hydroxylase (T7H, PDB ID: 5C3Q, Z-score: 31.8) of *Neurospora crassa*.<sup>36</sup> An overall structural comparison of TropC with *Pa/PNS* and T7H suggested a putative substrate binding site for TropC (Supplementary Figure S30). Overlaying TropC with T7H revealed several shared residues which define the substrate binding site in the T7H structure (Supplementary Figure S31).<sup>33</sup> Specifically, residues F284 and F213 align well with two conserved aromatic residues in T7H, F292 and Y217, respectively.<sup>33</sup> F292 and Y217 have been demonstrated as critical for substrate binding and alignment in T7H, with F292 providing  $\pi$ - $\pi$  stacking interactions that align thymine in the enzyme active site for productive catalysis.<sup>33</sup> The conservation of these aromatic residues in homologs of T7H and their alignment with F284 and F213 in TropC suggests that these residues may play an analogous role in substrate alignment.<sup>33</sup> In addition, bound metal ion was observed in the structure of TropC, which was refined to be Fe(III). As has been observed with the active site of other  $\alpha$ -KG-dependent NHI dioxygenases, our structure demonstrates that the conserved HxD/E...H metal binding residues are involved in interaction with Fe(II) <sup>33-34, 36</sup>. Specifically, our data showed the coordination of residues H210, D212 and H269 (located at the loop between  $\beta$ 4-5 and  $\beta$ 9) to the active site Fe(III) atom (Figure 3).

Crystallography experiments yielded vital information on structural features of TropC and enabled further investigation of mechanistic considerations by computational and mutagenic analysis. Toward this goal, we anticipated that an enzyme-substrate complex would provide critical information for determining the active site residues that are involved in ring expansion catalysis. To construct a computational substrate-bound model, we modeled the missing electron density from the C-terminus and used an overlaid structure of T7H to establish the coordinates of critical enzyme cofactors, such as  $\alpha$ -KG, ferrous iron and substrate (see Supplemental Information for model construction and simulation details). To prepare the model for substrate binding studies, we performed a molecular mechanics (MM) minimization over 5000 steps. The system was then prepared for a combined quantum mechanics and molecular dynamics (QM/MD) simulation. The system was subjected to three phases of MD simulations in which the system was heated, equilibrated, and sampled for a total of 12 ns to generate an enzyme-substrate-cosubstrate complex with the appropriate geometry and alignment for C-H atom abstraction (see Supplemental Information for details).

Our analysis of the substrate-bound TropC model revealed that substrate **10** was flanked by numerous active site residues that could potentially be involved in substrate binding or catalysis (Figure 4C). Residues from the TropC substrate pocket were identified and selected for alanine screening to determine if specific amino acids are critical for the ring expansion process. We anticipated that a TropC variant, without the required residue for a polar, semi-pinacol-type ring expansion, would be unable to generate stipitaldehyde, resulting in a change to the ratio of observed enzyme products toward formation of the shunt product, **18** (Figure 4A). We carried out mutagenesis of twelve active site residues, generating the corresponding alanine variants (Figure 4B and Supplementary Figure S2) as well as variants with isosteric and isoelectronic residues at the same position. These residues were chosen using the substrate-bound TropC model as a guide and were selected for their proximity to the substrate as well as their ability to participate in the proposed reaction pathways. Many of the resulting variants were soluble, but catalytically inactive, suggesting that the structural changes in

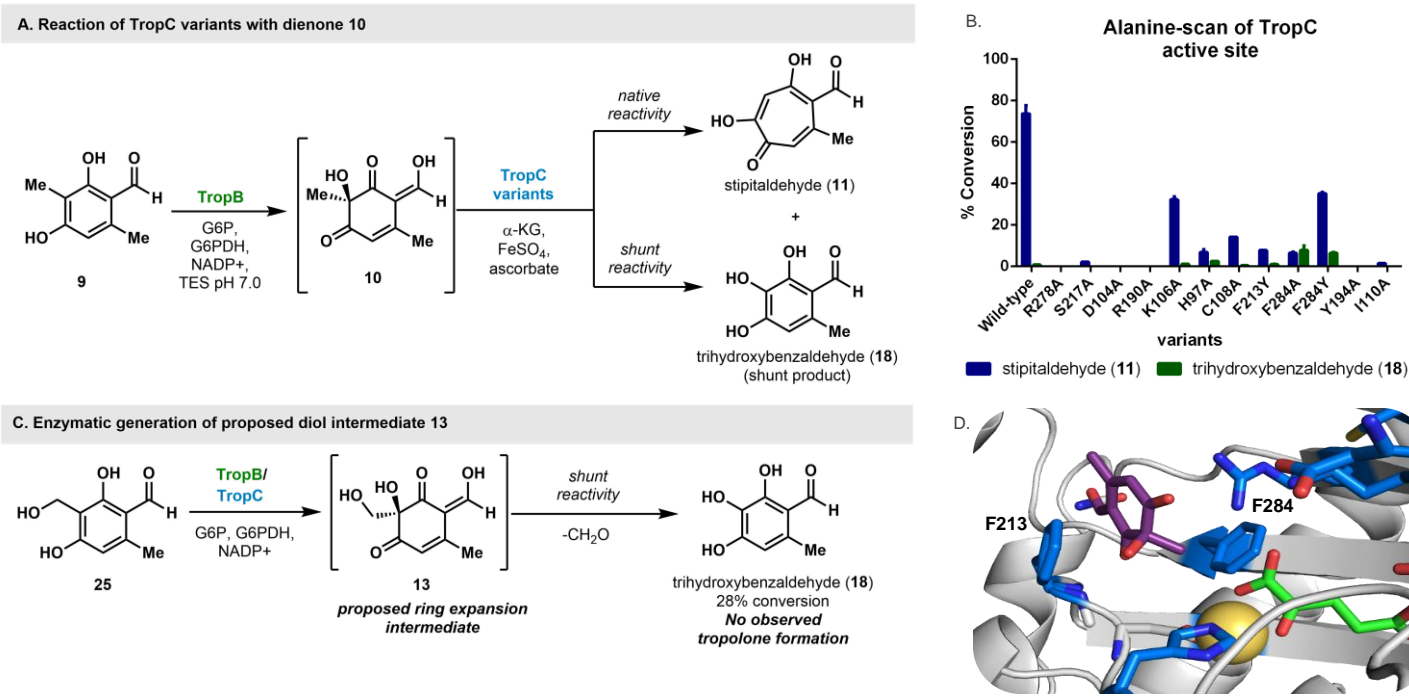


**Figure 4.** A. Oxidative dearomatization and ring expansion cascade to generate stipitaldehyde (**11**) and trihydroxybenzaldehyde (**18**). B. Product profiles observed in alanine-scanning of TropC active site residues. C. Enzymatic synthesis of proposed ring expansion intermediate, diol **10**. D. Close-up view of substrate-bound model of TropC with select targeted alanine-scanning residues highlighted in blue,  $\alpha$ -KG highlighted in green and the substrate shown in purple.

some variants prevented productive catalysis. Catalytically active variants exhibited reduced enzymatic conversion to products, but the product profiles were largely unaltered, and stipitaldehyde (**11**) remained the major product under the reaction conditions, suggesting that most of the substrate-flanking residues were not involved in catalysis. However, the F284A variant uniquely demonstrated a shift in the product profile to produce nearly equimolar amounts of stipitaldehyde (**11**) and trihydroxybenzaldehyde (**18**). Analysis of the substrate-bound TropC model suggests that this residue could be important for positioning of the substrate in the active site. This proposed role is analogous to the function of residue F292 in T7H, which has been shown to be critical for binding and alignment of substrate for productive catalysis. The binding mode of substrate **10** in the TropC MD simulation demonstrates that F284 and F213 flank the substrate in the active site, potentially guiding the proper alignment for C–H atom abstraction. This proposal is likewise analogous to the reported role of F292 and Y217 in T7H, suggesting a similar function in aligning the TropC substrate to achieve catalysis.<sup>33</sup> To further investigate this hypothesis, we generated the isosteric variant TropC F284Y which reconstituted the ring expansion activity of the enzyme, providing further evidence that F284 is a critical residue for determining the product mixtures generated by TropC. We aimed to further analyze this reaction by generating a TropC F213A variant but were unable to produce soluble protein with this construct. Despite this challenge, the data generated through alanine scanning of the TropC active site suggested that substrate alignment plays a role in determining the product profile of the enzyme. Perturbations of this alignment often result in a change to the products generated by the enzyme, providing clues about the mechanism of the transformation.<sup>7, 9</sup> In particular, substrate alignment relative to the iron(III)-hydroxyl species is key in discriminating whether rebound hydroxylation occurs over other NHI-catalyzed reactivity, such as halogenation.<sup>37</sup> In the context of our TropC model, these observations support the proposed mechanistic pathway for radical ring expansion (Path 1) in which the fate of the radical (rearrangement versus rebound hydroxylation) determines which product is generated by the enzyme. In addition, mutagenic changes to polar residues did not produce a corresponding shift in the product profile to the production of trihydroxybenzaldehyde **18**, suggesting that local acid or base catalysis does not drive a ring expansion mechanism (Figure 1D, Path 1).

We aimed to further interrogate the proposed semi-pinacol rearrangement (Figure 1D, Path 1) by evaluating the reactivity of the proposed diol intermediate **13**. To generate the target diol in the absence of TropC, a biocatalytic approach was employed using CitB and TropB.<sup>21, 27, 38-40</sup> We aimed to directly synthesize diol **13** through oxidative dearomatization of benzylic alcohol **25** using TropB. Notably, trihydroxybenzaldehyde **18** was detected in these reactions, but diol intermediate **13** was not observed, suggesting that the fragmentation reaction described in Path 3 (Figure 1D) occurs spontaneously under the reaction conditions. To further probe whether diol **13** is a ring expansion intermediate in TropC catalysis, we again performed a TropB-catalyzed oxidative dearomatization of benzylic alcohol **25** and included TropC in this reaction. We envisioned that diol **13**, when generated *in situ*, could enter the active site of TropC and undergo a ring expansion reaction

as proposed in reaction Path 2 (Figure 1D). In this reaction, exclusive formation of trihydroxybenzaldehyde (**18**) was observed with no stipitaldehyde (**11**) detected, suggesting that fragmentation and rearomatization of diol **13** is the predominant mode of reactivity observed for this putative intermediate (Figure 4D). In support of this finding, Riess and coworkers noted this same fragmentation and rearomatization reactivity in their attempts to perform ring expansion reactions on *ortho*-dearomatized phenols to produce tropolones (Supplementary Figure S29).<sup>41</sup> These observations also agree with the computational modelling which suggests that fragmentation and rearomatization is a low-barrier process (18.2 kcal/mol). Taken together, these data indicate that diol intermediate **13** is unlikely to be the correct ring expansion intermediate in the TropC-catalyzed reaction, further suggesting that a radical mechanism (Path 2) leads to tropolone formation in this NHI system.

## Conclusions

These experimental observations and QM calculations suggest that TropC-catalyzed ring expansion occurs through a radical-based process (Path 2), rather than the previously proposed rebound hydroxylation/semi-pinacol sequence (Path 1). This mechanistic proposal is supported by structural characterization, modelling and mutagenic analysis of the TropC active site, demonstrating that modification of a residue involved in substrate positioning altered the products generated by the enzyme. These data suggest that substrate positioning in TropC determines which radical termination step predominates: rebound hydroxylation or radical rearrangement followed by single electron transfer. Furthermore, we have demonstrated that rebound hydroxylation generates an intermediate (**13**) which does not undergo ring expansion, but rather a fragmentation and rearomatization process to produce trihydroxybenzaldehyde **18**. The observed reactivity of intermediate **13** illustrates the thermodynamic favorability for rearomatization over ring expansion in *ortho*-dearomatized phenols, as has been documented in previous studies.<sup>32, 41</sup> This revised proposal of radical-based ring expansion is also supported by literature precedent, demonstrating that tropolones can be synthesized from *ortho*-dearomatized radicals. These findings provide strong evidence of a radical-based mechanism for fungal tropolone biosynthesis, representing a major shift in the current understanding of the role of NHI enzymes in this process. In addition, our observations provide new insight into the mechanistic processes harnessed by NHI enzymes for the selective synthesis of complex molecules. We anticipate that computational studies that consider active site geometries could provide additional insight into these transformations and the observed behavior of TropC variants. Furthermore, we envision that the molecular details of NHI-catalyzed ring expansion can be leveraged to address current challenges in the synthesis of tropolone natural product scaffolds.

## Acknowledgements

This work was supported by funds from the University of Michigan Life Sciences Institute and Department of Chemistry. T.J.D. thanks the National Science Foundation for a Graduate Research Fellowship. K.C.S acknowledges a Rackham Merit Fellowship from the University of Michigan Rackham Graduate School. P.M.Z. acknowledges partial support from NIH R35GM128830.

## References

1. Walsh, C. T.; Moore, B. S., Enzymatic Cascade Reactions in Biosynthesis. *Angew. Chem. Intl. Ed.* **2019**, *58* (21), 6846-6879.
2. Klas, K.; Tsukamoto, S.; Sherman, D. H.; Williams, R. M., Natural Diels–Alderses: Elusive and Irresistible. *J. Org. Chem.* **2015**, *80* (23), 11672-11685.
3. Christianson, D. W., Structural and Chemical Biology of Terpenoid Cyclases. *Chem. Rev.* **2017**, *117* (17), 11570-11648.
4. Herr, C. Q.; Hausinger, R. P., Amazing Diversity in Biochemical Roles of Fe(II)/2-Oxoglutarate Oxygenases. *Trends. Biochem. Sci.* **2018**, *43* (7), 517-532.
5. Dowd, P.; Zhang, W., Free radical-mediated ring expansion and related annulations. *Chem. Rev.* **1993**, *93* (6), 2091-2115.
6. Donald, J. R.; Unsworth, W. P., Ring-Expansion Reactions in the Synthesis of Macrocycles and Medium-Sized Rings. *Chem. Eur. J.* **2017**, *23* (37), 8780-8799.
7. Bai, J.; Yan, L.; Liu, Y., Catalytic mechanism of the PrhA (V150L/A232S) double mutant involved in the fungal meroterpenoid biosynthetic pathway: a QM/MM study. *Phys. Chem. Chem. Phys.* **2019**, *21* (46), 25658-25668.
8. Matsuda, Y.; Iwabuchi, T.; Fujimoto, T.; Awakawa, T.; Nakashima, Y.; Mori, T.; Zhang, H.; Hayashi, F.; Abe, I., Discovery of Key Dioxygenases that Diverged the Paraherquonin and Acetoxydehydroaustin Pathways in *Penicillium brasilianum*. *J. Am. Chem. Soc.* **2016**, *138* (38), 12671-7.
9. Nakashima, Y.; Mori, T.; Nakamura, H.; Awakawa, T.; Hoshino, S.; Senda, M.; Senda, T.; Abe, I., Structure function and engineering of multifunctional non-heme iron dependent oxygenases in fungal meroterpenoid biosynthesis. *Nat. Commun.* **2018**, *9* (1), 104.

10. Nakamura, H.; Matsuda, Y.; Abe, I., Unique chemistry of non-heme iron enzymes in fungal biosynthetic pathways. *Nat. Prod. Rep.* **2018**, *35* (7), 633-645.
11. Kovaleva, E. G.; Lipscomb, J. D., Versatility of biological non-heme Fe(II) centers in oxygen activation reactions. *Nat. Chem. Biol.* **2008**, *4* (3), 186-93.
12. Timmins, A.; Visser, S. P. d., A Comparative Review on the Catalytic Mechanism of Nonheme Iron Hydroxylases and Halogenases. *Catalysts* **2018**, *8* (8).
13. Martinez, S.; Hausinger, R. P., Catalytic Mechanisms of Fe(II)- and 2-Oxoglutarate-dependent Oxygenases. *J. Biol. Chem.* **2015**, *290* (34), 20702-11.
14. Yan, L.; Liu, Y., Insights into the Mechanism and Enantioselectivity in the Biosynthesis of Ergot Alkaloid Cycloclavine Catalyzed by Aj\_EasH from *Aspergillus japonicus*. *Inorg. Chem.* **2019**, *58* (20), 13771-13781.
15. Jakubczyk, D.; Caputi, L.; Stevenson, C. E. M.; Lawson, D. M.; O'Connor, S. E., Structural characterization of EasH (*Aspergillus japonicus*) – an oxidase involved in cycloclavine biosynthesis. *Chem. Commun.* **2016**, *52* (99), 14306-14309.
16. Tarhonskaya, H.; Szöllössi, A.; Leung, I. K. H.; Bush, J. T.; Henry, L.; Chowdhury, R.; Iqbal, A.; Claridge, T. D. W.; Schofield, C. J.; Flashman, E., Studies on Deacetoxycephalosporin C Synthase Support a Consensus Mechanism for 2-Oxoglutarate Dependent Oxygenases. *Biochemistry* **2014**, *53* (15), 2483-2493.
17. Valegard, K.; Terwisscha van Scheltinga, A. C.; Dubus, A.; Ranghino, G.; Oster, L. M.; Hajdu, J.; Andersson, I., The structural basis of cephalosporin formation in a mononuclear ferrous enzyme. *Nat. Struct. Mol. Biol.* **2004**, *11* (1), 95-101.
18. Jakubczyk, D.; Caputi, L.; Hatsch, A.; Nielsen, C. A.; Diefenbacher, M.; Klein, J.; Molt, A.; Schroder, H.; Cheng, J. Z.; Naesby, M.; O'Connor, S. E., Discovery and reconstitution of the cycloclavine biosynthetic pathway--enzymatic formation of a cyclopropyl group. *Angew. Chem. Int. Ed. Engl.* **2015**, *54* (17), 5117-21.
19. Cox, R., Oxidative rearrangements during fungal biosynthesis. *Nat. Prod. Rep.* **2014**, *31* (10), 1405-24.
20. Cox, R. J.; Al-Fahad, A., Chemical mechanisms involved during the biosynthesis of tropolones. *Curr. Opin. Chem. Biol.* **2013**, *17* (4), 532-6.
21. Davison, J.; al Fahad, A.; Cai, M.; Song, Z.; Yehia, S. Y.; Lazarus, C. M.; Bailey, A. M.; Simpson, T. J.; Cox, R. J., Genetic, molecular, and biochemical basis of fungal tropolone biosynthesis. *Proc. Natl. Acad. Sci. U. S. A.* **2012**, *109* (20), 7642-7.
22. Liu, N.; Song, W.; Schienebeck, C. M.; Zhang, M.; Tang, W., Synthesis of Naturally Occurring Tropones and Tropolones. *Tetrahedron* **2014**, *70* (49), 9281-9305.
23. Reisman, S. E.; Nani, R. R.; Levin, S., Buchner and Beyond: Arene Cyclopropanation as Applied to Natural Product Total Synthesis. *Synlett* **2011**, *2011* (17), 2437-2442.
24. Stevens, H. C.; Reich, D. A.; Brandt, D. R.; Fountain, K. R.; Gaughan, E. J., A New Tropolone Synthesis via Dichloroketene. *Journal of the American Chemical Society* **1965**, *87* (22), 5257-5259.
25. Barbier, M.; Barton, D. H. R.; Devys, M.; Topgi, R. S., A simple synthesis of tropones and related compounds. *Tetrahedron* **1987**, *43* (21), 5031-5038.
26. Barbier, M.; Barton, D. H. R.; Devys, M.; Topgi, R. S., A simple synthesis of the tropone nucleus. *J. Chem. Soc. Chem. Commun.* **1984**, (12), 743-744.
27. Abood, A.; Al-Fahad, A.; Scott, A.; Hosny, A. E.-D. M. S.; Hashem, A. M.; Fattah, A. M. A.; Race, P. R.; Simpson, T. J.; Cox, R. J., Kinetic characterisation of the FAD dependent monooxygenase TropB and investigation of its biotransformation potential. *RSC Adv.* **2015**, *5* (62), 49987-49995.
28. Schor, R.; Schotte, C.; Wibberg, D.; Kalinowski, J.; Cox, R. J., Three previously unrecognised classes of biosynthetic enzymes revealed during the production of xenovulene A. *Nat. Commun.* **2018**, *9* (1), 1963.
29. Zhai, Y.; Li, Y.; Zhang, J.; Zhang, Y.; Ren, F.; Zhang, X.; Liu, G.; Liu, X.; Che, Y., Identification of the gene cluster for bistropolone-humulene meroterpenoid biosynthesis in *Phoma* sp. *Fungal Genet. Biol.* **2019**, *129*, 7-15.
30. Cho, K.-B.; Hirao, H.; Shaik, S.; Nam, W., To rebound or dissociate? This is the mechanistic question in C–H hydroxylation by heme and nonheme metal–oxo complexes. *Chem. Soc. Rev.* **2016**, *45* (5), 1197-1210.
31. Timmins, A.; Fowler, N. J.; Warwicker, J.; Straganz, G. D.; de Visser, S. P., Does Substrate Positioning Affect the Selectivity and Reactivity in the Hectochlorin Biosynthesis Halogenase? *Front. Chem.* **2018**, *6* (513).
32. Borowski, T.; Wójcik, A.; Miłaczewska, A.; Georgiev, V.; Blomberg, M. R. A.; Siegbahn, P. E. M., The alkenyl migration mechanism catalyzed by extradiol dioxygenases: a hybrid DFT study. *J. Biol. Inorg. Chem.* **2012**, *17* (6), 881-890.
33. Li, W.; Zhang, T.; Ding, J., Molecular basis for the substrate specificity and catalytic mechanism of thymine-7-hydroxylase in fungi. *Nucleic Acids Res.* **2015**, *43* (20), 10026-10038.
34. Aik, W.; McDonough, M. A.; Thalhammer, A.; Chowdhury, R.; Schofield, C. J., Role of the jelly-roll fold in substrate binding by 2-oxoglutarate oxygenases. *Curr. Opin. Struct. Biol.* **2012**, *22* (6), 691-700.
35. Holm, L.; Rosenstrom, P., Dali server: conservation mapping in 3D. *Nucleic Acids Res* **2010**, *38* (Web Server issue), W545-9.
36. Zhang, H.; Che, S.; Wang, R.; Liu, R.; Zhang, Q.; Bartlam, M., Structural characterization of an isopenicillin N synthase family oxygenase from *Pseudomonas aeruginosa* PAO1. *Biochem. Biophys. Res. Commun.* **2019**, *514* (4), 1031-1036.

37. Mitchell, A. J.; Dunham, N. P.; Bergman, J. A.; Wang, B.; Zhu, Q.; Chang, W. C.; Liu, X.; Boal, A. K., Structure-Guided Reprogramming of a Hydroxylase To Halogenate Its Small Molecule Substrate. *Biochemistry* **2017**, *56* (3), 441-444.
38. Doyon, T. J.; Perkins, J. C.; Baker Dockrey, S. A.; Romero, E. O.; Skinner, K. C.; Zimmerman, P. M.; Narayan, A. R. H., Chemoenzymatic o-Quinone Methide Formation. *J. Am. Chem. Soc.* **2019**, *141* (51), 20269-20277.
39. Baker Dockrey, S. A.; Lukowski, A. L.; Becker, M. R.; Narayan, A. R. H., Biocatalytic site- and enantioselective oxidative dearomatization of phenols. *Nat. Chem.* **2018**, *10* (2), 119-125.
40. He, Y.; Cox, R. J., The molecular steps of citrinin biosynthesis in fungi. *Chem. Sci.* **2016**, *7* (3), 2119-2127.
41. Cacioli, P.; Reiss, J., Reactions of 1-Oxaspiro[2.5]octa-5,7-dien-4-ones with nucleophiles. *Aust. J. Chem.* **1984**, *37* (12), 2525-2535.